THE GEOLOGICAL SOCIETY OF AMERICA®

Pore fluids in Dead Sea sediment core reveal linear response of lake chemistry to global climate changes

Elan J. Levy[1,2], Mordechai Stein[2,3], Boaz Lazar[3], Ittai Gavrieli[2], Yoseph Yechieli[2,4], and Orit Sivan[1]
[1]Department of Geological and Environmental Sciences, Ben-Gurion University of the Negev, Beer Sheva 8410501, Israel
[2]Geological Survey of Israel, 30 Malkhe Israel Street, Jerusalem 95501, Israel
[3]The Fredy & Nadine Herrmann Institute of Earth Sciences, The Hebrew University of Jerusalem, Edmond J. Safra Campus, Givat Ram, Jerusalem 91904, Israel
[4]Department of Hydrology and Microbiology, Zuckerberg Center, Ben-Gurion University of the Negev, Sede Boker 8499000, Israel

ABSTRACT

Pore fluids extracted from a 456 m sediment core, recovered within the framework of a multinational and International Continental Scientific Drilling Program (ICDP) co-sponsored effort at the bottom of the terminal Dead Sea, recorded the chemical variations in the deep lake over the past 220 k.y. Mg^{2+} and Br^- were shown to be conservative in the pore fluids, increasing in concentration during interglacial periods, diluting during glacials, and providing excellent proxies for deep lake net water balance changes. Furthermore, the Na/Cl ratio recorded the process of halite precipitation and dissolution induced by these hydrological changes. Mg^{2+} and Br^- records follow a glacial-interglacial pattern, such as observed in atmospheric CO_2 concentrations and global sea-surface temperatures, albeit with a phase offset. At the end of the last interglacial (ca. 116 ka), there is a delay in onset of dilution of the deep lake, most likely due to the limnological transition from holomictic to meromictic conditions. The increase in deep lake concentrations at Last Glacial Termination I is delayed as a result of freshwater input into the deep lake during the cooler Younger Dryas period. There is a persistent relationship between precipitation in the watershed and North Atlantic sea-surface temperatures, similar to conditions observed over the past instrumental record. Deviations from the long-term trends occurred during interglacial periods, Marine Isotope Stages MIS 5e and MIS 1, when the deep Dead Sea was significantly diluted, and coincided with Mediterranean sapropel layers S5 and S1.

INTRODUCTION

The Dead Sea, a terminal hypersaline lake, situated in a deep tectonic basin along the Dead Sea transform, receives its water from a large (~40,000 km^2) watershed, extending between the desert belt and the Mediterranean climate zone in the central Levant region. Its main freshwater source is from precipitation into the watershed during winter cyclonic activity (Cyprus lows) from the East Mediterranean region (Enzel et al., 2003). Observations of 19th- and 20th-century precipitation in the region display a multidecadal relationship between the Mediterranean-related precipitation and North Atlantic (NA) sea-surface temperature (SST) variability, such that when the North Atlantic was relatively cold, the region had relatively high precipitation, and, conversely, when warm, had relatively low precipitation (Kushnir and Stein, 2010). As regional precipitation was positively correlated with lake levels during the instrumental period, the NA SST–regional climate connection could be further extended and applied to the late Holocene Dead Sea lake level curve (Kushnir and Stein, 2010).

Dead Sea lake level records, along with lithological properties of the sediments deposited at the margins, all show evidence of regional climate variability over time. This evidence suggests a close relationship of the lake with both short- and long-term NA climate patterns during the past 70 k.y. (Bartov et al., 2003; Haase-Schramm et al., 2004; Prasad et al., 2004; Stein et al., 2010; Torfstein et al., 2013). However, these records from the lake margins are discontinuous, with several depositional gaps and hiatuses. These omissions were addressed by the 2010–2011 International Continental Scientific Drilling Program (ICDP) Dead Sea Deep Drilling Project (DSDDP) drilling of a long sediment core at the deep Dead Sea floor (300 m water column depth), which unearthed an almost complete sedimentary record spanning 220 k.y. (Stein et al., 2011; Neugebauer et al., 2014; Torfstein et al., 2015). This core, studied for its lithological and chemical compositions, indicated significant differences between glacial and interglacial periods (Neugebauer et al., 2014; Lazar et al., 2014; Kiro et al., 2016). Sediments pertaining to the last glacial and penultimate glacial periods (Marine Isotope Stage [MIS] MIS 6 and MIS 4–2) comprise mainly sequences of alternating aragonite ($CaCO_3$) and fine detritus (of the *aad* facies), layered gypsum ($CaSO_4 \cdot 2H_2O$), and laminated detrital marl (*ld*). In addition, sediments of the two most recent interglacial periods (MIS 5 and 1) comprise mainly fine detritus in the form of laminated detrital marl (*ld*) together with considerable quantities of layered halite (NaCl) (Neugebauer et al., 2014). Riddled with low-permeability evaporite deposits and fine detrital material, the core provides a unique opportunity for evaluating the chemical evolution of the deep lake from pore fluids. In our previous work using Cl^- and $\delta^{18}O_{H_2O}$, we showed that the last-glacial deep lake salinity had undergone dilution, possibly due to turbulent mixing along an internal stratified interface (Lazar et al., 2014). Here, we present selected conservative and non-conservative chemical records from pore fluids taken along the ICDP core that have directly and indirectly recorded the net water balance changes in the deep lake over 220 k.y., changes that were controlled by the most significant regional climate activity over this interval.

METHODS

A description of the ICDP drilling project at the Dead Sea and details of core 5017-1-A (at 31°30′28.98″N, 35°28′15.60″E), retrieved during November 2010 to March 2011, are given by Neugebauer et al. (2014). Pore fluids were extracted from fine detrital sediment samples taken along the core at intervals averaging ~3.5 m and ranging from several centimeters to 14.5 m. A total of 126 pore fluid analyses were performed: 96 from core catchers and 30 from core sections. Core catcher samples were extracted immediately following core collection. Sediment handling and post-extraction pore fluid treatment followed preparations described in Lazar et al. (2014). Core section sediment samples of 15 ml were taken at the Helmholtz Centre Potsdam GFZ German Research Centre for Geosciences during July 2012, and fluid was extracted using a hydraulic press extraction system before immediate analysis for chemical compositions (see Table DR1 in the GSA Data Repository[1]). Modern Dead Sea deep lake

[1]GSA Data Repository item 2017093, methods, supplemental information, Figures DR1–DR4, and Tables DR1–DR3, is available online at http://www.geosociety.org/datarepository/2017/ or on request from editing@geosociety.org.

concentrations measured prior to anthropogenic-induced lake overturn during the late 1970s were compared to those of pore fluids (Steinhorn, 1985). Major cations (Na^+ and Mg^{2+}) were analyzed using inductively coupled plasma–atomic emission spectroscopy (ICP-AES), Br^- using ICP-MS, and Cl^- by titration, with a charge balance error (C.B.E.) ±<5%, at the Geological Survey of Israel (Jerusalem). The relative conservativeness of Mg^{2+} and Br^- was assessed, and any samples displaying non-conservative behavior were removed from the records (Item DR1 in the Data Repository). Based on a combination of the core anchor age model (Torfstein et al., 2015) and ^{14}C from plants (Neugebauer et al., 2014), core depth–to–age conversion was implemented (Item DR2; Fig. DR1 in the Data Repository; Table DR3). The effect of pore fluid diffusion over 220 k.y. was quantified using a one-dimensional diffusive transport model (Item DR3 ; Fig. DR3). Additionally, phase analysis of Mg^{2+} and Br^- relative to the composite CO_2 record from Antarctic ice cores (Lüthi et al., 2008) was carried out (Item DR4; Table DR2).

DILUTION AND CONCENTRATION OF THE DEEP LAKE

The Mg^{2+} and Br^- concentration records show similar trends to one another (Figs. 1A and 1B; Fig. DR1). During evaporation or dilution of Dead Sea water, these ions remain conservative, until the precipitation of the evaporative mineral carnallite ($KMgCl_3{\cdot}6H_2O$) at a degree of evaporation of ~1.67 relative to modern Dead Sea water (Gavrieli et al., 1989), a value not encountered in the pore fluids (Item DR1; Fig. DR2). Subsurface physical transport processes are capable of significantly modifying pore fluid Mg^{2+} and Br^- concentration profiles. Thus, one-dimensional forward diffusive transport modeling was carried out to estimate deep paleolake concentrations, so-called "pre-diffusion" concentrations (Item DR3; Fig. DR3; Fig. 1B). Based on the model results, between 89 and 0 mblf (meters below lake floor) and between 320 and 200 mblf, there is minimal concentration modification as a result of abundant impermeable halite layers present in these intervals. Thus pore fluid concentrations over these depths are similar to values found in the deep Dead Sea at that time (Fig. 1B). Between ~199 and 90 mblf, there are no halite layers, and diffusion has smoothed out most of the short-term (millennial-scale) variability while retaining the long-term trend. In the lower section of the core, however, between ~455 and 321 mblf, there is significant modification, which makes it difficult to estimate deep lake concentrations accurately.

Assuming no change in the Mg^{2+} and Br^- molar inventory over time, net water balance changes in the deep lake relative to the modern Dead Sea can be estimated by dividing Dead Sea Mg^{2+} and Br^- concentrations [mol kg $(H_2O)^{-1}$] by pore fluid Mg^{2+} and Br^- concentrations (giving the term "degree of dilution," or DD_{Mg} and DD_{Br}; Item DR1). The estimations can be representative for either the deep lake or the whole lake, depending on whether the Dead Sea was stratified (meromictic) or not (holomictic), respectively, hence the use of the term *minimum* DD, which emphasizes that the lake at any given point in time could potentially have been more diluted than these estimates (Fig. 1B).

As noted previously, Mg^{2+} and Br^- concentration records show similar trends, as expected of conservative ions (Figs. 1A and 1B). An interesting feature is that the trends appear to show a mirror image in comparison to Na/Cl (Fig. 1C; Fig. DR1). Where the Mg^{2+} and Br^- concentrations increase, there is a decrease in Na/Cl, and vice versa. During evaporation of Dead Sea water and precipitation of halite, there is progressive removal of Na^+ and Cl^- at a ratio of 1:1, and as Na/Cl < 1 in the modern and ancient Dead Sea, there is a decrease in Na/Cl in the residual brine. Indeed it will be shown that layered halite in the core appears alongside a decrease in Na/Cl in the pore fluids. An increase in Na/Cl, however, can be indicative of halite dissolution, which occurs in the lake when the water becomes undersaturated with respect to halite because of dilution. To summarize, the net water balance changes instigated a mechanism of dissolution and precipitation of halite, which is recorded in the Na/Cl ratio. This finding is important for three reasons:

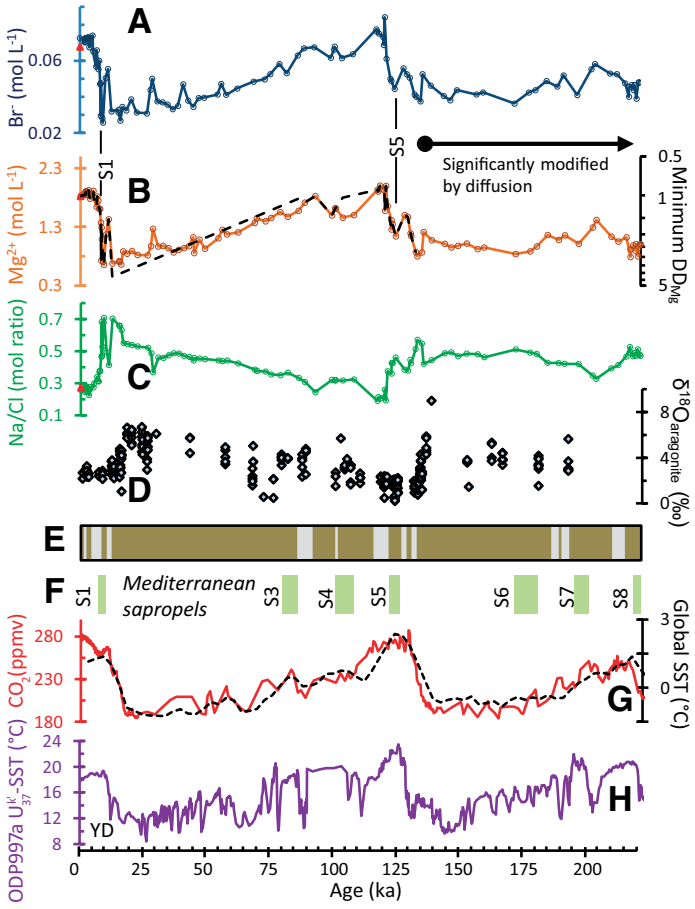

Figure 1. Comparison of Dead Sea Deep Drilling Project core 5017-1-A pore fluid chemistry to sediments, marine, and global proxies. A: Pore fluid Br^- concentrations (mol L^{-1}). B: Pore fluid Mg^{2+} concentrations (mol L^{-1}). Pre-diffusion concentrations estimated from diffusion modeling (Item DR3 [see footnote 1]) are shown by the black dashed line. Right *y*-axis (log scale) projects estimates for minimum degree of dilution, DD_{Mg}. C: Na/Cl. In A, B, and C, modern Dead Sea concentrations (pre–1970s overturn; Steinhorn, 1985) are red triangles. D: $\delta^{18}O_{aragonite}$ (‰) from core sediments (Torfstein et al., 2015). E: Simplified core lithology. Halite layers are shown in gray, non-halite sediments in brown. Full lithological section can be found in Figure DR1 (see footnote 1). F: Mediterranean sapropel layers (S1–S7). G: Composite CO_2 record (ppmv) from Antarctic ice cores (Lüthi et al., 2008) and superimposed global sea-surface temperature (SST) stack record (Shakun et al., 2015). H: SST based on $U^{k'}_{37}$ alkenone ratio record from marine sediment core ODP Hole 161-977a at the western Mediterranean Sea (Martrat et al., 2004) (NA—North Atlantic; YD—Younger Dryas).

(1) Na/Cl can be used as a separate, non-conservative proxy for dilution/concentration.

(2) Dilution or concentration of Mg^{2+} and Br^- in the deep Dead Sea is independent of salinity dilution or concentration. There is a "salinity buffering" mechanism as a result of precipitation or dissolution of halite.

(3) A decrease in Na/Cl should be concurrent with the presence of halite layers in the core and can be used to correlate pore fluids to the core sedimentary record.

Although significantly modified by diffusion over most of the penultimate glacial period between ca. 190 and 132 ka (393–316 mblf), the deep lake was diluted by a factor of ~2–2.5 relative to the modern Dead Sea (Fig. 1B). From ca. 132 to 127 ka (~316–301 mblf), the conservative ion concentrations increased while the Na/Cl ratio decreased, along with appearance of halite layers (Figs. 1A–1C and 1E); together this is indicative of a shift to low lake level stands (Kiro et al., 2016). Toward the end

of this period, at ca. 128 ka and 303 mblf, is the base of a thick silt layer with interspersed aragonite laminae deposited until ca. 122 ka (280 mblf) (Torfstein et al., 2015), and Mg^{2+} and Br^- concentrations had become diluted. From ca. 122 to 117/116 ka (~279–235 mblf), once again Mg^{2+} and Br^- concentrations increased while the Na/Cl ratio decreased, and a thick sequence of halite is present. At these depths, the minimum DD_{Mg} is ~0.9. Significantly, between ca. 116 and 12.5 ka, there was a general long-term dilution of Mg^{2+} and Br^- concentrations and an enrichment of Na^+ and Cl^- as a result of halite dissolution. Over this period, there is evidence of several millennial-scale increases in Mg^{2+} and Br^- concentrations, such as at ca. 92–85 ka (~210–200 mblf), together with a decrease in Na/Cl and, once again, the presence of a sequence of halite. Following these intervals, the long-term dilution trend prevailed. At the end of this >100 k.y. interval, the deep lake was diluted by a factor of >4, when accounting for diffusion. Following deposition of a halite layer at ca. 11.4 ka (88.5 mblf), the Mg^{2+} and Br^-increased in concentration and the Na/Cl ratio significantly decreased. Mg^{2+} and Br^- concentrations were briefly but significantly diluted within a sedimentary interval largely composed of laminated detrital material (*ld*) and *aad* facies, sandwiched between halite layers dated at 9.5–8.7 ka (70.5–63.7 mblf). Following this dilution interval, there was a transition back to high Mg^{2+} and Br^- concentrations, similar to values found in the pre-overturn deep Dead Sea.

THE NORTH ATLANTIC–DEAD SEA CLIMATE CONNECTION

The Mg^{2+} and Br^- records show, quite strikingly, a long-term glacial-interglacial pattern, similar to the composite CO_2 record from Antarctic ice cores (Lüthi et al., 2008) and global SST stack record (Shakun et al., 2015) (Fig. 1G). The SST record, based on $U^{k'}_{37}$ alkenone ratios from the ODP Hole 161-977a marine core at the westernmost portion of the Mediterranean Sea, the Alboran sea (Martrat et al., 2004; Fig. 1H) has millennial- and multimillennial-scale variability but also carries a prominent glacial-interglacial signal with relatively warmer SST during interglacial in comparison to glacial periods. Although it appears as if the net water balance changes in the deep lake closely follow the long-term global climate variations observed in the global records, a more thorough investigation reveals discrepancies. There are two periods of dilution found in the Dead Sea core, at ca. 128–122 ka and 9.5–8.7 ka, which are not significantly evident in the global records. These two intervals correlate to Mediterranean sapropel layers S5 and S1, dated at 128.3–121.5 ka and at 10.5–6.1 ka, respectively (Grant et al., 2016; Fig. 1F).

Mediterranean sapropel layers are organic-rich sediments likely formed by anoxia induced by increased freshwater input from North African river catchment systems during the intensification and migration of the summer African monsoon (e.g., Grant et al., 2016). Within the southern region of the Dead Sea watershed, the Negev desert, and Arava valley, there was sporadic deposition of travertines and speleothems at ages corresponding to those of the sapropel layers, which were suggested to be formed as a result of intrusion of southern-source precipitation, probably in association with enhanced activity of mid-latitude Red Sea synoptic troughs and/or low-latitude tropical plumes (Waldmann et al., 2010). Indeed, in the ICDP core, there is evidence of increased fluvial derived detrital and/or siliciclastic input into the lake, corresponding to the last-interglacial sapropel S5 (Torfstein et al., 2015) as well as at depths corresponding to S3 and S4 (Neugebauer et al., 2016). Moreover, during the early Holocene, there is some evidence of lake level rise from the marginal terraces at ca. 10–9 ka (Stein et al., 2010). Dated Holocene wood fragments, found in flood sediments in elevated salt caves, also point to high lake levels at, and prior to, ca. 8 ka (Frumkin et al., 1994), possibly correlative to Mediterranean sapropel S1 (Robinson et al., 2006).

Plots of 1-k.y.-interpolated Mg^{2+} and Br^- concentrations against the CO_2 record show a typical shape of a Lissajous ellipse, revealing phase offsets of Mg^{2+} and Br^- after CO_2 (Fig. 2A; Item DR4; Table DR2). It is assumed that values pertaining to the two dilution events, at ca. 128–122 ka and between 9.5 and 8.7 ka, reflect regional phenomena, as they significantly deviate from the CO_2 trends. Shifting the interpolated Br^- record back in time by ~4 k.y. transforms the ellipse into a linear fit with a correlation coefficient, $r(123) = 0.89$ (Fig. 2B). For ease of explanation, the ellipse has been split into intervals 1–5 (Fig. 2A).

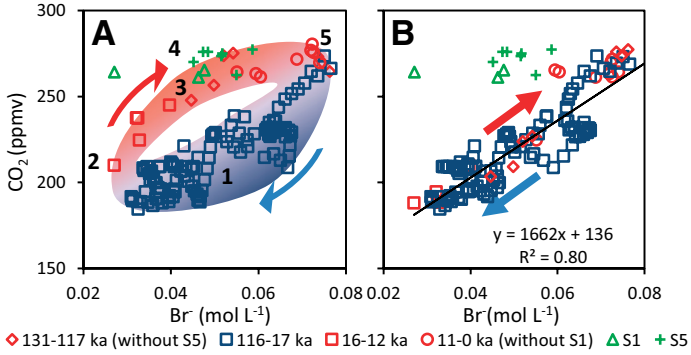

Figure 2. Interpolated pore fluid Br^- (mol L^{-1}) verus CO_2 (Lüthi et al., 2008) over 132 k.y. Green symbols correspond to Mediterranean sapropel layers S1 and S5. A: No forced phase offset. Intervals 1–5 are shown on plot (see text for explanation). B: Phase offset of Br^- backward by 4 k.y. yields reasonable linear trend (excluding data points corresponding to Mediterranean sapropels S1 and S5).

Interval 1 spans ca. 116–17 ka from the end of MIS 5e to Termination I. Over this period, Br^- shows a trend of reducing concentration with a concurrent decrease in CO_2, but with substantial variability. This interval represents the long-term dilution of the deep brine, most likely during stratified meromictic conditions instigated by a strong density gradient between dense hypersaline brine and overlying freshwater-controlled epilimnion (Lazar et al., 2014). Interval 2, which spans 16–12 ka, shows an increase in CO_2, however Br^- continues to be diluted. Indeed, in addition to the increase in CO_2 and global warming of SST at this time interval, the $\delta^{18}O_{aragonite}$ from the ICDP core (Torfstein et al., 2015) also shows depletion earlier than the increase in conservative ion concentration and the onset of halite, which appears at the end of Termination I following the Younger Dryas period (see Figs 1A, 1B, and 1D; Fig. DR4). The Younger Dryas period, a global cold spell occurring between 12.9 and 11.7 ka and observed by a drop in ODP 977a SST (Fig. 1F; Fig. DR4), occurred simultaneously with this interval. The transition of interval 2 to interval 3 occurs at the onset of a layer of halite at ca. 11.4 ka (at 88.5 mblf), the first one in the core since ca. 85 ka. Interval 3 on the ellipse covers most of the last interglacial and Holocene periods, where there is a concurrent increase in CO_2 and Br^- concentrations. However, these periods are punctuated by significant dilution events which correspond to Mediterranean sapropels S1 and S5 (interval 4), which deviate from the Lissajous ellipse. Interval 5, marking the end of MIS 5e (120–117 ka), is characterized by a decrease in CO_2, while Br^- shows no apparent change and remains highly concentrated. Unlike the delay of Br^- relative to CO_2 in interval 2, which can be explained by a continuous positive net water balance into the deep lake during the Younger Dryas period, at interval 5 the delay might be the result of kinetic constraints of deep lake dilution that are instigated by the transition from holomictic to meromictic conditions (interval 1). However, the apparent delay of deep lake freshening is not apparent at interval 4 (i.e., the dilution events correspond to S1 and S5). Thus, it could be that regional climate characteristics, such as source, intensity, and proximity of precipitation in the watershed, play a role in the onset and magnitude of deep lake dilution, although more research is needed to test this hypothesis.

Given the documented relationship between precipitation in the region and NA SST over the past instrumental record (Kushnir and Stein, 2010),

the relationship can now be projected over a full interglacial–glacial–last interglacial cycle, and possibly beyond. At times of cool NA SST there is an increased net water balance in the lake. Conversely, during periods of warm NA SST, there is a decreased net water balance. Indeed the SST based on the $U^{k'}_{37}$ alkenone ratio record has features that support this proposed climate mechanism, namely both glacial-interglacial trends and cooler waters during the Younger Dryas period. The long-term NA SST–regional precipitation relationship appears to be persistent, however there are periods where it was significantly disturbed when there was enhanced hydrological influx concurrent with monsoon activity in the sub-Sahara African Sahel and in association with Mediterranean sapropels.

SUMMARY

Net water balance changes of the deep Dead Sea were recorded in the pore fluid chemistry, both directly and indirectly, and show a glacial-interglacial sawtooth wave pattern. At Termination I, the deep Dead Sea continued to be diluted with respect to Mg^{2+} and Br^- until the end of the Younger Dryas period. Together, these observations point to a persistent long-term relationship between NA SST and regional precipitation from the Mediterranean region, similar to conditions found over the past instrumental record (Kushnir and Stein, 2010). This relationship was briefly disturbed, probably by precipitation from southern sources, at intervals concurrent with Mediterranean sapropels S1 and S5.

ACKNOWLEDGMENTS

We thank the editor, anonymous reviewers, and C.B. de Wet for thelping to significantly improve the paper. We wish to sincerely thank I. Swaed from the Geological Survey of Israel (GSI), E. Eliani-Russak, M. Adler, I. Bar-Or, N. Avrahamov, and A. Russak from Ben-Gurion University of the Negev, and G. Antler from Aarhus University for help in core catcher sampling and analysis. D. Stiber, G. Sharabi, and other members in the GSI geochemical division carried out major ion analysis. We thank I. Neugebauer, M. Schwab, and R. Conze from GFZ Potsdam and others on the Dead Sea Deep Drilling Project team during pore fluid sampling; and J. Kallmeyer and J. Axel Kitte from the University of Potsdam for help in pore fluid extraction. We thank A. Turchyn for fruitful discussion, and L. Monaghan for proofreading. The study is supported by an Excellence Center of the Israel Science Foundation grant 1736/11 to Lazar.

REFERENCES CITED

Bartov, Y., Goldstein, S., Stein, M., and Enzel, Y., 2003, Catastrophic arid episodes in the Eastern Mediterranean linked with the North Atlantic Heinrich events: Geology, v. 31, p. 439–442, doi:10.1130/0091-7613(2003)031<0439:CAEITE>2.0.CO;2.

Enzel, Y., Bookman, R., Sharon, D., Gvirtzman, H., Dayan, U., Ziv, B., and Stein, M., 2003, Late Holocene climates of the Near East deduced from Dead Sea level variations and modern regional winter rainfall: Quaternary Research, v. 60, p. 263–273, doi:10.1016/j.yqres.2003.07.011.

Frumkin, A., Carmi, I., Zak, I., and Magaritz, M., 1994, Middle Holocene environmental change determined from the Salt Caves of Mount Sodom, Israel, *in* Bar-Yosef, O., and Kra, R.S., eds., Late Quaternary Chronology and Paleoclimates of the Eastern Mediterranean: Tucson, University of Arizona Press, p. 315–332.

Gavrieli, I., Starinsky, A., and Bein, A., 1989, The solubility of halite as a function of temperature in the highly saline Dead Sea brine system: Limnology and Oceanography, v. 34, p. 1224–1234, doi:10.4319/lo.1989.34.7.1224.

Grant, K.M., Grimm, R., Mikolajewicz, U., Marino, G., Ziegler, M., and Rohling, E.J., 2016, The timing of Mediterranean sapropel deposition relative to insolation, sea-level and African monsoon changes: Quaternary Science Reviews, v. 140, p. 125–141, doi:10.1016/j.quascirev.2016.03.026.

Haase-Schramm, A., Goldstein, S.L., and Stein, M., 2004, U-Th dating of Lake Lisan (late Pleistocene Dead Sea) aragonite and implications for glacial east Mediterranean climate change: Geochimica et Cosmochimica Acta, v. 68, p. 985–1005, doi:10.1016/j.gca.2003.07.016.

Kiro, Y., Goldstein, S.L., Lazar, B., and Stein, M., 2016, Environmental implications of salt facies in the Dead Sea: Geological Society of America Bulletin, v. 128, p. 824–841, doi:10.1130/B31357.1.

Kushnir, Y., and Stein, M., 2010, North Atlantic influence on 19th–20th century rainfall in the Dead Sea watershed, teleconnections with the Sahel, and implication for Holocene climate fluctuations: Quaternary Science Reviews, v. 29, p. 3843–3860, doi:10.1016/j.quascirev.2010.09.004.

Lazar, B., Sivan, O., Yechieli, Y., Levy, E.J., Antler, G., Gavrieli, I., and Stein, M., 2014, Long-term freshening of the Dead Sea brine revealed by porewater Cl^- and $\delta^{18}O$ in ICDP Dead Sea deep-drill: Earth and Planetary Science Letters, v. 400, p. 94–101, doi:10.1016/j.epsl.2014.03.019.

Lüthi, D., et al., 2008, High-resolution carbon dioxide concentration record 650,000–800,000 years before present: Nature, v. 453, p. 379–382, doi:10.1038/nature06949.

Martrat, B., Grimalt, J.O., López-Martinez, C., Cacho, I., Sierro, F.J., Flores, J.A., Zahn, R., Canals, M., Curtis, J.H., Hodell, D.A., 2004, Abrupt temperature changes in the western Mediterranean over the past 250,000 years: Science, v. 306, p. 1762-1765, doi:10.1126/science.1101706.

Neugebauer, I., et al., 2014, Lithology of the long sediment record recovered by the ICDP Dead Sea Deep Drilling Project (DSDDP): Quaternary Science Reviews, v. 102, p. 149–165, doi:10.1016/j.quascirev.2014.08.013.

Neugebauer, I., et al., 2016, Hydroclimatic variability in the Levant during the early last glacial (~117–75 ka) derived from micro-facies analyses of deep Dead Sea sediments: Climate of the Past, v. 12, p. 75–90, doi:10.5194/cp-12-75-2016.

Prasad, S., Vos, H., Negendank, J.F.W., Waldmann, N., Goldstein, S.L., and Stein, M., 2004, Evidence from Lake Lisan of solar influence on decadal- to centennial-scale climate variability during marine oxygen isotope stage 2: Geology, v. 32, p. 581–584, doi:10.1130/G20553.1.

Robinson, S.A., Black, S., Sellwood, B.W., and Valdes, P.J., 2006, A review of palaeoclimates and palaeoenvironments in the Levant and Eastern Mediterranean from 25,000 to 5000 years BP: Setting the environmental background for the evolution of human civilization: Quaternary Science Reviews, v. 25, p. 1517–1541, doi:10.1016/j.quascirev.2006.02.006.

Shakun, J.D., Lea, D.W., Lisiecki, L.E., and Raymo, M.E., 2015, An 800-kyr record of global surface ocean $\delta^{18}O$ and implications for ice volume-temperature coupling: Earth and Planetary Science Letters, v. 426, p. 58–68, doi:10.1016/j.epsl.2015.05.042.

Stein, M., Torfstein, A., Gavrieli, I., and Yechieli, Y., 2010, Abrupt aridities and salt deposition in the post-glacial Dead Sea and their North Atlantic connection: Quaternary Science Reviews, v. 29, p. 567–575, doi:10.1016/j.quascirev.2009.10.015.

Stein, M., Ben-Avraham, Z., and Goldstein, S.L., 2011, Dead Sea deep cores: A window into past climate and seismicity: Eos (Transactions, American Geophysical Union), v. 92, p. 453–454, doi:10.1029/2011EO490001.

Steinhorn, I., 1985, The disappearance of the long term meromictic stratification of the Dead Sea: Limnology and Oceanography, v. 30, p. 451–472, doi:10.4319/lo.1985.30.3.0451.

Torfstein, A., Goldstein, S., Stein, M., and Enzel, Y., 2013, Impacts of abrupt climate changes in the Levant from Last Glacial Dead Sea levels: Quaternary Science Reviews, v. 69, p. 1–7, doi:10.1016/j.quascirev.2013.02.015.

Torfstein, A., Goldstein, S.L., Kushnir, Y., Enzel, Y., Haug, G., and Stein, M., 2015, Dead Sea drawdown and monsoonal impacts in the Levant during the last interglacial: Earth and Planetary Science Letters, v. 412, p. 235–244, doi:10.1016/j.epsl.2014.12.013.

Waldmann, N., Torfstein, A., and Stein, M., 2010, Northward intrusions of low- and mid-latitude storms across the Saharo-Arabian belt during past interglacials: Geology, v. 38, p. 567–570, doi:10.1130/G30654.1.

Manuscript received 22 May 2016
Revised manuscript received 9 December 2016
Manuscript accepted 10 December 2016

Printed in USA